A photoionization study of trifluoromethanol, CF_3OH, trifluoromethyl hypofluorite, CF_3OF, and trifluoromethyl hypochlorite, CF_3OCl

Robert L. Asher, Evan H. Appelman, Jeffrey L. Tilson, Maritoni Litorja, Joseph Berkowitz, and Branko Ruscic
Argonne National Laboratory, Argonne, Illinois 60439-4831

(Received 26 November 1996; accepted 7 March 1997)

CF_3OH, an important and controversial by-product of atmospheric decomposition of CF_3CFH_2 (HFC-134a) and other hydrofluorocarbons, has been examined by photoionization mass spectrometry. The ionization onset is characterized by a broad Franck–Condon distribution, arising primarily from a substantial elongation of the C–O bond upon ionization. An upper limit to the adiabatic ionization potential (IP) of $\leqslant 13.08 \pm 0.05$ eV has been established. The appearance potentials (APs) of the first two fragments have been accurately determined by fitting with appropriate model functions as $AP_0(CF_2OH^+/CF_3OH) \leqslant 13.830 \pm 0.005$ eV and $AP_0(CF_3^+/CF_3OH) \leqslant 13.996 \pm 0.005$ eV. While the exact nature of the lowest-energy fragment (nominally CF_2OH^+) is not clear, the CF_3^+ fragment threshold leads unambiguously to $\Delta H^\circ_{f\,298}(CF_3OH) \geqslant -217.2 \pm 0.9$ kcal/mol and $D_{298}(CF_3\text{–}OH) \leqslant 115.2 \pm 0.3$ kcal/mol. With previously derived $\Delta H^\circ_{f\,298}(CF_3O) = -151.8^{+1.7}_{-1.1}$ kcal/mol, this yields $D_{298}(CF_3O\text{–}H) = 117.5^{+1.9}_{-1.4}$ kcal/mol, very close to, or only slightly weaker than the O–H bond energy in water: $D_{298}(CF_3O\text{–}H) - D_{298}(HO\text{–}H) = -1.8^{+1.9}_{-1.4}$ kcal/mol ≈ 0 kcal/mol. Similarly, with the recently redetermined value for $\Delta H^\circ_f(CF_2O)$, this implies a 298 K reaction enthalpy for the 1,2-elimination of HF from CF_3OH of $2.8^{+1.7}_{-1.1}$ kcal/mol. CF_3OF and CF_3OCl have also been examined by photoionization. CF_3OF produces a very weak parent, with an apparent adiabatic $IP(CF_3OF) \leqslant 12.710 \pm 0.007$ eV. An analysis of the CF_3^+ and CF_2O^+ fragments from CF_3OF, when combined with literature data, suggests $\Delta H^\circ_{f\,298}(CF_3OF) = -176.9^{+1.8}_{-1.3}$ kcal/mol. The fitted value for the appearance potential of CF_3^+ from CF_3OCl, $AP_0(CF_3^+/CF_3OCl) \leqslant 12.85 \pm 0.01$ eV, leads to $\Delta H^\circ_{f\,298}(CF_3OCl) \geqslant -175.6 \pm 1.0$ kcal/mol, $D_{298}(CF_3\text{–}OCl) \leqslant 88.4 \pm 0.3$ kcal/mol, and $D_{298}(CF_3O\text{–}Cl) \leqslant 52.8^{+2.0}_{-1.5}$ kcal/mol. © *1997 American Institute of Physics.* [S0021-9606(97)03122-X]

I. INTRODUCTION

Hydrofluorocarbons (HFCs) and hydrochlorofluorocarbons (HCFCs) are generally perceived as environmentally friendlier alternatives to chlorofluorocarbons (CFCs) and halons (bromofluorocarbons and bromochlorofluorocarbons), which have been implicated in the anthropogenic depletion of stratospheric ozone.[1] The general idea is that most of the fluorine ends up bound as HF, thus having little effect on the ozone budget.[2] However, it has been established recently that oxidative degradation of HFC-134a (CF_3CFH_2), HFC-143a (CF_3CH_3), HFC-125 (CF_3CF_2H), HFC-23 (CF_3H), HCFC-123 (CF_3CCl_2H), and others can produce CF_3 radicals. By reaction with O_2 or NO, these are readily converted[3] to CF_3O, which may be involved in catalytic ozone removal cycles.[4] Although recent studies strongly suggest that the relevant rate coefficients are low,[4(b),5] the ozone depletion potential of HFCs ultimately depends on how efficiently CF_3O can be removed from the damaging cycle. Among various possibilities, a prominent group of chain-termination reactions are those that convert CF_3O to CF_3OH by hydrogen abstraction from suitable donors, such as hydrocarbons[6] and perhaps even water.[7,8] The ultimate fate of stratospheric CF_3OH is not clear at this time; however, it has been shown that it has a very long lifetime with respect to unimolecular decomposition[9] ($> 10^4$ yr) or photolysis[10] ($\sim 10^6$ yr), with a significantly shorter lifetime with respect to heterogeneous decomposition in the troposphere.[11] Thus, it appears that the strength of the O–H bond energy is an important factor in determining whether CF_3OH is a good sink for stratospheric CF_3, or merely a long-lived reservoir.

From experimental observations on chlorine-initiated decomposition of HFC-134a, Wallington *et al.* recently[7] concluded that CF_3O radicals react with H_2O, producing CF_3OH and OH, suggesting that the O–H bond energy in CF_3OH must be comparable to that in water, i.e., $D_{298}(CF_3O\text{–}H) = 120 \pm 3$ kcal/mol. This surprisingly high value seems to be corroborated by a number of theoretical studies.[7,12–18] However, as Benson[19] pointed out, there is a significant volume of experimental data[20] which, when combined with bond additivity[19,20] and other empirical estimates,[19] appears to firmly establish $D_{298}(CF_3O\text{–}H) = 109 \pm 2.5$ kcal/mol (see Table I and also Ref. 21). The basic disagreement of $\sim$ 10–11 kcal/mol between the ''low'' and the ''high'' bond energy arises from the fact that the theoretical $\Delta H^\circ_f(CF_3OH)$ is *lower* by $\sim 2-7$ kcal/mol than the empirical value, while $\Delta H^\circ_f(CF_3O)$ is *higher* by $\sim 2-8$ kcal/mol than the values suggested by the experiments.

In trying to resolve this issue by theoretical means, Montgomery *et al.*[16(a)] and Schneider and Wallington[17] have shown that a significant portion of the discrepancy stems from the fact that the *ab initio* value $\Delta H^\circ_f(CF_2O) = -145.3 \pm 1.7$ kcal/mol, is $\sim$ 7 kcal/mol higher than the

TABLE I. Review of literature values for $D_{298}(CF_3O–H)$, $\Delta H^\circ_{f\,298}(CF_3OH)$, and $\Delta H^\circ_{f\,298}(CF_3O)$ (all in kcal/mol).

$D_{298}(CF_3O–H)$	$\Delta H^\circ_{f\,298}(CF_3OH)$	$\Delta H^\circ_{f\,298}(CF_3O)$	Source
120 ± 3	⋯	⋯	Wallington *et al.*[a]
119.4 ± 2	-217.7 ± 2	-150.4 ± 2	Schneider and Wallington[b]
⋯	-217.4	⋯	Sana *et al.*[c]
119.4 ± 1.5	⋯	⋯	Dixon and Fernandez[d]
$111.8-121.9$	⋯	⋯	Bock *et al.*[e]
⋯	-217.7 ± 2	⋯	Montgomery *et al.*[f]
~119	-217.7 ± 2.0	-149.2 ± 2.0	Schneider and Wallington[g]
118.2	-220.7	-154.5	Schneider *et al.*[h]
109	-213.5 ± 1.5	-156.7 ± 1.5	Batt and Walsh[i]
109 ± 2.5	-215 ± 1	-157 ± 1.5	Benson[j]
⋯	⋯	-155.4 ± 1.1	Schneider *et al.*[k]
124.7 ± 3.6	⋯	⋯	Huey *et al.*[l]

[a]Reference 7, based on the experimental observation that CF_3O radicals react with H_2O and supported by *ab initio* calculations at the MP4 level.
[b]Reference 12, theoretical value at the MP4 level.
[c]Reference 13, theoretical value.
[d]Reference 14, theoretical value.
[e]Reference 15(b); the range is obtained by combining theoretical values at the MP4 level from Ref. 15(a) with experimental bond energies for CH_4, C_2H_6, and H_2O.
[f]Reference 16(a), based on the theoretical value at the G2 level and isogyric reaction schemes.
[g]Recommended values from Ref. 17, based on a combination of various theoretical calculations and experimental data from Ref. 20.
[h]Reference 18, theoretical values at the MP2 level.
[i]Reference 20; $\Delta H^\circ_f(CF_3O)$ is derived from a variety of experimental data, while $\Delta H^\circ_f(CF_3OH)$ is estimated from bond additivity.
[j]Reference 19, reiterating data from Ref. 20 and adding another estimate for $\Delta H^\circ_f(CF_3OH)$ based on homothermicity of OH and F.
[k]Reference 21, reiterating experimental data from Ref. 20, but avoiding the use of JANAF's value for $\Delta H^\circ_f(CF_3OF)$.
[l]From L. G. Huey, E. J. Dunlea, and C. J. Howard, J. Phys. Chem. **100**, 6504 (1996); the bond energy is based on experimental gas-phase acidity $\Delta_{acid}H^\circ_{298}(CF_3OH)=329.8\pm2.0$ kcal/mol and an estimated electron affinity $EA(CF_3O)=108.5\pm3.0$ kcal/mol.

JANAF[22] value, $\Delta H^\circ_{f\,298}(CF_2O)=-152.7\pm0.4$ kcal/mol, to which the experimental[19,20] $\Delta H^\circ_f(CF_3O)$ is referred. The claim that the generally accepted tabulated value,[22,23] which is based on a determination of the enthalpy of hydrolysis (quoted to $\pm$ 0.2 kcal/mol) and other experimental measurements, is in error by such a significant amount, has been recently investigated by us.[24] Our photoionization study of CF_2O yielded $\Delta H^\circ_{f\,298}(CF_2O)\geqslant-149.1^{+1.4}_{-0.7}$ kcal/mol and indicated unequivocally (since ours is a strict lower limit) that the tabulated[22,23] value is indeed too low, albeit only by 3–4 kcal/mol. However, our study also implied that the theoretical values[16(a),17] are most likely too high by 3–4 kcal/mol, which brings into question the accuracy of calculated heats of formation for other fluorine-rich compounds, including CF_3OH. Curtiss *et al.*[25] have very recently performed a reassessment of GAUSSIAN-2 (G2) and density functional theories (DFT) and concluded that the largest deviations between experiment and theory tend to occur for molecules having multiple fluorine atoms.

The best approach to solve this puzzle is to provide independent experimental evaluations of either $D_{298}(CF_3O–H)$ or $\Delta H^\circ_{f\,298}(CF_3OH)$. Although CF_3OH has long been considered to belong to a category of compounds that were too unstable to be prepared in bulk, Seppelt and his colleagues[26] succeeded in synthesizing this material and reported that it had some measure of kinetic stability at subambient temperatures. Therefore, it appeared to us that it might be feasible to examine this compound by photoionization mass spectroscopy. To this end we have undertaken the present study.

II. EXPERIMENT

The photoionization apparatus employed in this study was described recently in some detail.[24] The present experiments utilized primarily the He Hopfield continuum and, in a few instances, the many-lined Werner and Lyman emission bands of H_2. The nominal photon resolution was 0.84 Å (full width at half-maximum). All measurements of light intensity were performed via a sodium salicylate transducer coupled to an external photomultiplier. The H_2 lines, or, in the case of He Hopfield continuum, the superimposed Ne I, N II, and H I lines provided an accurate internal wavelength calibration. The uncertainty in the wavelength scale depends on the density of experimental points, and is believed to be accurate to $\pm$ 0.2 Å in most spectra presented here.

Trifluoromethanol, CF_3OH, was prepared by the reaction of trifluoromethyl hypochlorite, CF_3OCl, with HCl in

$CClF_3$ solvent as the mixture was gradually warmed from liquid-nitrogen temperature to $-100\,^{\circ}C$.[26(b)] The reaction was carried out in a 3/4 in.-o.d. Kel-F tube fitted with a Kel-F needle valve. The solvent and excess HCl were removed by pumping at $-130\,^{\circ}C$, and the Cl_2 by-product at $-100\,^{\circ}C$. Trifluoromethanol was stored at liquid-nitrogen temperature in the reaction vessel. No decomposition was observed even after many days of storage.

Trifluoromethyl hypochlorite, CF_3OCl, and trifluoromethyl hypofluorite, CF_3OF, were prepared by the cesium-fluoride-catalyzed addition of ClF and F_2, respectively, to carbonyl fluoride, CF_2O, at temperatures between $-78\,^{\circ}C$ and ambient.[27] For both preparations, the anhydrous CsF catalyst was dried before use by heating in an atmosphere of F_2. The catalyst was mixed with 3/16-in.-diam stainless steel balls in a Monel reaction vessel to permit effective agitation. The product was distilled from the reaction vessel into a Monel pressure vessel, in which it was stored at ambient temperature. No decomposition of either compound was observed during storage.

Technical-grade CF_2O was obtained from PCR, Inc. and ClF from Ozark–Mahoning. Chlorotrifluoromethane, $CClF_3$, and anhydrous HCl were obtained from AGA Specialty Gases, and anhydrous cesium fluoride was purchased from Aldrich.

The flow of CF_3OH into the photoionization apparatus was controlled by regulating the temperature of the sample vessel with a suitable slush bath, rather than by throttling with a valve. The best results were obtained with a slush of ''aged'' methanol, which had picked up some moisture from the air and, depending on its composition, could hold a stable temperature between -98 and $-104\,^{\circ}C$ throughout the day. During our initial attempt to admit the CF_3OH into the instrument, we were only able to detect the decomposition products CF_2O and HF. By making successive modifications to the inlet system, we were able to improve significantly the ratio of CF_3OH to its decomposition products. The changes consisted of shortening as much as possible the transport path from the sample vessel to the ionization region, as well as removing all metal surfaces from the sample path and replacing them with components fabricated from Teflon™ or Kel-F. In the process we learned that even the smallest and seemingly unimportant metal components (such as a 2-cm-long piece of 1/4-in.-o.d. tubing inside the vacuum, at the inlet of the ionization cell) can cause considerable decomposition of CF_3OH.

Both the trifluoromethylhypochlorite, CF_3OCl, and the trifluoromethylhypofluorite, CF_3OF, were admitted directly into the instrument from their Monel storage cylinders. The sample pressure was reduced by cooling the cylinder in an appropriate slush bath; acetone/dry-ice ($-78\,^{\circ}C$) was used for CF_3OCl; and *n*-pentane ($-131\,^{\circ}C$) for CF_3OF. The sample flow was further controlled by a relatively coarse inlet needle valve. Since CF_3OCl was causing a very rapid deterioration of the particle multiplier, the number of measurements performed with this sample was kept to a bare minimum.

III. COMPUTATIONAL DETAILS

The supporting *ab initio* calculations on CF_3OH were performed using the GAUSSIAN 94 package.[28] Geometries of neutral and ionic species were optimized at the MP2 (second-order Møller–Plesset) level using the 6-31 G(d,p) basis set.[29] Prior to use, the calculated harmonic frequencies were scaled by 0.89.

The thermodynamically relevant experimental fragmentation thresholds were obtained by least-squares fits of the data with appropriate model functions. This approach has been shown to produce appearance potentials of significantly greater accuracy and reliability than graphical extrapolation methods.[24,30,31] The relevant details of this method have been presented recently elsewhere.[24] The model functions used here have been obtained by convoluting a flexible kernel of the form $\{1-\exp[-B(h\nu-E_T)]\}$ with an internal energy distribution function of the form $E^{\eta}\exp(-aE)$, where $h\nu$ is the photon energy, E_T is the fragmentation threshold, and B, η, and a are adjustable parameters.[24] Parameter η of the function representing the internal energy distribution of the neutral parent was predetermined with the aid of Haarhoff's expression[32] for the density of states, computed numerically in the range of interest by using either calculated (CF_3OH), experimental[33] (CF_3OF), or estimated (CF_3OCl) frequencies.[34] Parameter a was obtained by imposing the requirement that the overall function corresponds to the correct amount of average internal energy available for fragmentation at 298 K (0.090 eV for CF_3OH, 0.113 eV for CF_3OF, and ~ 0.12 eV for CF_3OCl). In most cases where the model function provides an adequate description of the observed threshold, and the statistical scatter of the experimental points is small or moderate, the quality of the fit (as determined by the Gaussian criterion) is a surprisingly sensitive function of the threshold value E_T, with an associated uncertainty similar to, and often even smaller, than the uncertainty in the wavelength calibration.

IV. RESULTS

A. Overview and parent ionization of CF_3OH

Table II lists a typical mass spectrum of CF_3OH observed at the He I resonance line at 584.33 Å (21.218 eV). The intensities are not corrected for the inherent mass discrimination function of the quadrupole mass spectrometer. A fraction of $m/e = 66$ (CF_2O^+), and essentially all of $m/e = 20$ (HF^+) can be attributed to ionization of CF_2O and HF, since some CF_3OH was heterogeneously decomposing in the inlet in spite of all precautions. Using the ratio of signals[24] at $m/e = 66$ and 47 from pure CF_2O, one concludes that no more than 1/3 of $m/e = 47$ (FCO^+) in Table II can be attributed to fragmentation of CF_2O. Therefore, CF_3^+ and FCO^+ are the two most prominent fragments from CF_3OH, followed by CF_2OH^+. Parent ionization contributes less than 10% to the total ionization.

The He I mass spectrum in Table II shows that $m/e = 85$ (CF_3O^+ fragment) is at the lower limit of detectability. This frustrates the most direct approach to determine

TABLE II. A typical photoionization mass spectrum of the CF_3OH sample at 584.33 Å ≡ 21.218 eV. The intensities are not corrected for the quadrupole mass discrimination function.

m/e	Species	Relative intensity
86	CF_3OH^+	11.5
85	CF_3O^+	$<0.0_5$
69	CF_3^+	91.1
67	CF_2OH^+	39.6
66	CF_2O^+	[10.9][a]
50	CF_2^+	3.7[b]
47	FCO^+	100.0[c]
20	HF^+	6.1[d]

[a]Heavily contaminated by CF_2O from heterogeneous unimolecular decomposition of CF_3OH.
[b]Up to 1/4 of this intensity may be due to fragmentation from the decomposition product CF_2O.
[c]Not more than 1/3 of this intensity is due to fragmentation of the decomposition product CF_2O.
[d]Mostly from heterogeneous unimolecular decomposition of CF_3OH.

$D_0(CF_3O–H)$, which would have been to determine the appearance potential (AP) of the CF_3O^+ fragment from CF_3OH, and to combine it with a separately determined ionization potential (IP) of CF_3O, i.e., $D_0(CF_3O–H) = AP_0(CF_3O^+/CF_3OH) - IP(CF_3O)$. This approach would also have to account for the possibility that the $m/e = 85$ fragment can correspond to the isomeric (and likely more stable) CF_2OF^+. The fact that fragmentation to CF_2OF^+ requires rearrangement, while CF_3O^+ may be less favored energetically, is probably the inherent reason for the weakness of $m/e = 85$ fragment.

The next best approach to obtain $D(CF_3O–H)$ is to determine $\Delta H_f^\circ(CF_3OH)$ from the appearance potential of a suitable fragment. Table II suggests that CF_3^+ is probably the best candidate for this purpose. Of the other fragments, the heat of formation of CF_2OH^+ is less well established, while CF_2O^+ and FCO^+ are very difficult to use because of concomitant signals from the decomposition product CF_2O, which occur at slightly lower energy. Furthermore, FCO^+ from CF_3OH corresponds to a second-generation fragment, and is not a prime candidate for thermodynamical inferences.

Figure 1 shows an overview of the photoion yield signals obtained from CF_3OH between ~ 950 and 650 Å. The relative intensities of the ion yield curves reflect the true abundances as measured through our quadrupole mass filter. The FCO^+ signal is corrected for the contribution arising from fragmentation of CF_2O, while the relatively small signals corresponding to CF_2O^+ and HF^+ (~ 1/12 and ~ 1/16 of the CF_3^+ intensity at ~ 750 Å, respectively) are omitted altogether. They were interpreted as arising predominantly from parent ionization of the heterogeneous decomposition products, because their shapes matched rather closely known spectra of CF_2O and HF.

Figure 1 shows that parent ionization of CF_3OH corresponds to a relatively small overall contribution. The CF_3OH^+ yield attains its maximum at ~ 900 Å and, after a slight decline, maintains essentially a constant intensity as one proceeds to shorter wavelengths. Both CF_2OH^+ and

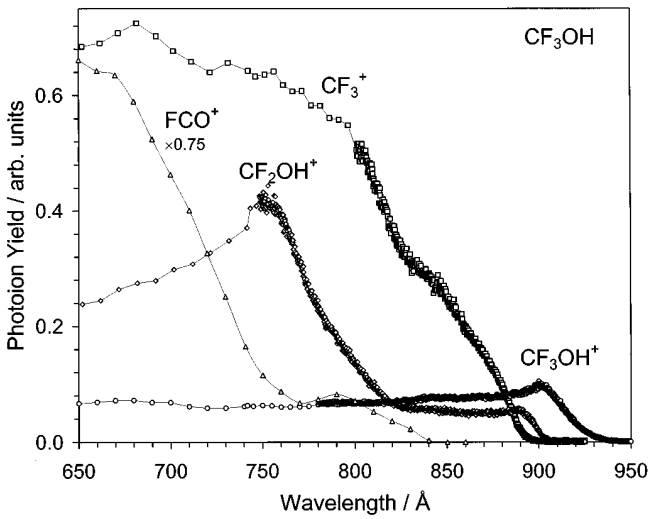

FIG. 1. An overview of the photoion yield curves of the parent CF_3OH^+ and its principal fragments, covering ~ 950–650 Å. At shorter wavelength only sparse points have been recorded. The relative abundance of all species is correctly depicted in the figure, apart from quadrupole transmission factors. The relatively small signals corresponding to CF_2O^+ and HF^+ (~ 1/12 and ~ 1/16 of the CF_3^+ intensity at ~ 750 Å, respectively) were omitted, since they were attributable to parent ionization of the heterogeneous decomposition products ($CF_3OH \rightarrow CF_2O + HF$). The FCO^+ signal shown is corrected for the contribution arising from fragmentation of CF_2O.

CF_3^+ appear relatively early, at ~ 900 Å. Figure 2 displays the threshold regions of CF_3OH^+, CF_2OH^+, and CF_3^+ in greater detail. From its onset, which appears to be rather rounded, the CF_3OH^+ parent ion keeps growing toward shorter wavelength until it culminates in a cusp (~ 902 Å), at which point the CF_2OH^+ fragment starts appearing. The

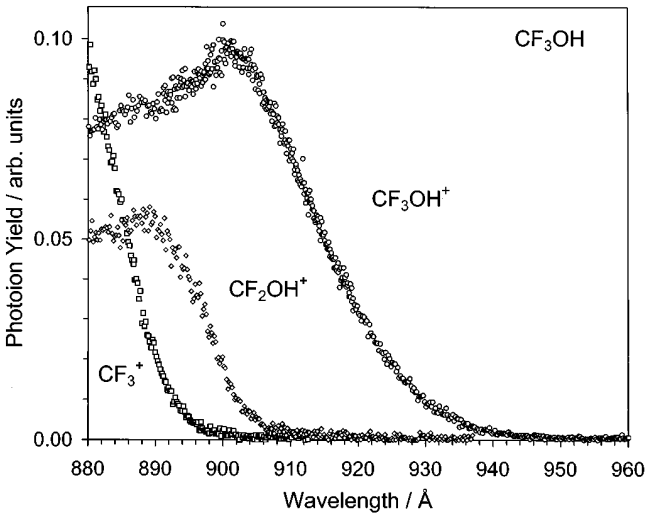

FIG. 2. The threshold regions of CF_3OH^+, CF_2OH^+, and CF_3^+ from CF_3OH. The parent ion displays a rounded onset, which is a consequence of a significant change in geometry upon ionization. The adiabatic threshold can be muddled by the presence of hot bands, which may be difficult to distinguish from vanishingly small Franck–Condon factors. Toward shorter wavelength, the growth of CF_3OH^+ terminates in a cusp coinciding with the onset of the first fragment, CF_2OH^+, which experiences a similar effect at the onset of the next fragment, CF_3^+.

TABLE III. MP2/6-31G(d,p) optimized geometries of CF_3OH and CF_3OH^+ and scaled harmonic vibrational frequencies.[a]

	CF_3OH	CF_3OH^+
r(CO)/Å	1.351	1.651
r(CF′)/Å	1.332	1.279
r(CF)/Å	1.352	1.290
r(OH)/Å	0.966	0.997
∠F′CO/°	108.3	102.2
∠FCO/°	112.2	102.3
∠COH/°	108.1	112.0
∠F′COH/°	180.0	180.0
Frequencies/cm^{-1}	3468	3146
	1302	1366
	1200	907
	1116	1311
	1026	842
	810	664
	564	354
	555	504
	535	503
	403	286
	391	291
	[208][b]	[63][b]

[a]Calculated harmonic frequencies are scaled by a factor of 0.89.
[b]Frequency corresponding to internal rotation.

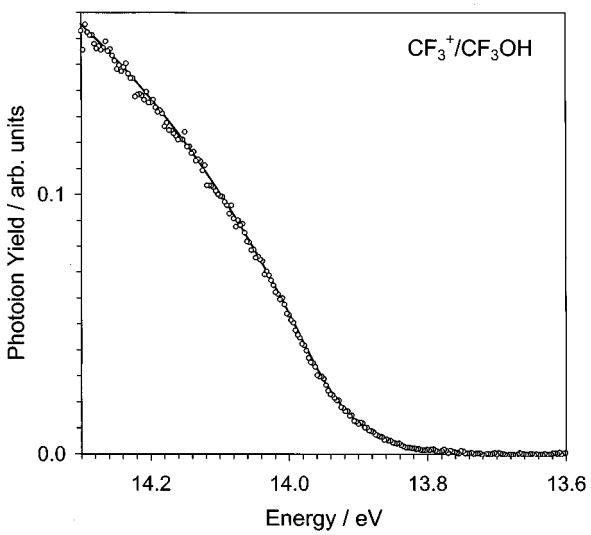

FIG. 3. The threshold region of the CF_3^+ fragment from CF_3OH. The solid line is a least-squares fit with a threshold model function (see the text) yielding $AP_0(CF_3^+/CF_3OH) \leqslant 13.996 \pm 0.005$ eV.

growth of CF_2OH^+ is, in turn, terminated in a cusp related to the onset of the CF_3^+ fragment. Such a pattern, where growth is stopped rather suddenly at the onset of the subsequent fragmentation process, can be interpreted as a sign that the internal energy of the parent is well randomized and that quasi equilibrium theory provides an adequate description of the unimolecular decomposition. Thus, the fragmentation onsets of both CF_2OH^+ and CF_3^+ look promising in providing thermodynamically useful information.

The pronouncedly rounded onset of the parent is an indication of a broad Franck–Condon envelope, reflecting a significant change in geometry upon ionization. Upon close scrutiny of several independent scans, it was determined that the first detectable departure of the parent ion signal from the background level occurs at 951 ± 2 Å $\equiv 13.04 \pm 0.03$ eV. This would nominally correspond to an upper limit to $IP(CF_3OH)$, if one were to disregard possible obfuscation from hot bands.

The importance of hot bands and the nature of the change in geometry upon ionization was further investigated by theoretical methods. The predicted adiabatic IP of 12.65 eV ≈ 980 Å (at the MP2 level and including zero-point energy corrections) is much lower than the experimentally observed onset. The vertical IP is predicted to occur ~ 0.95 eV higher (13.60 eV ≈ 910 Å), implying a very broad Franck– Condon envelope. Table III lists MP2 optimized geometries and scaled frequencies for CF_3OH and its cation. The values for the neutral species are similar to those published previously.[16] The calculated geometries indicate that ionization causes a considerable increase (0.300 Å) in the C–O bond length, and is expected to cause extended progressions of ~ 660 and 350 cm^{-1}. Based on the calculated changes in geometry, and assuming that the normal modes in the ion correspond to orthogonal harmonic oscillators,[35] we constructed a simulated Franck–Condon envelope. Surprisingly, the influence of room-temperature hot bands was relatively minor, and appeared to shift the apparent threshold toward lower energy only by ~ 0.04 eV. Therefore, correcting the experimental onset by a similar amount yields a conservative upper limit of $IP(CF_3OH) \leqslant 13.08 \pm 0.05$ eV.

B. The CF_3^+ and CF_2OH^+ fragments from CF_3OH

Figure 3 displays the threshold region of the CF_3^+ fragment in more detail. The solid line is a least-squares fit with a threshold model function, obtained as outlined in Sec. III. The fitted threshold value is $AP_{298}(CF_3^+/CF_3OH) \leqslant 13.906 \pm 0.005$ eV ($\leqslant 13.996 \pm 0.005$ eV at 0 K).

Figure 4 shows the threshold region of the CF_2OH^+ fragment in more detail. As opposed to the threshold region of the CF_3^+ fragment, CF_2OH^+ appears to display a weak sloping tail, extending to lower energy. The fit (the solid line in Fig. 4) accommodates for this by incorporating a linear background, with the relevant parameters obtained by prefitting the tail region between 13.2 and 13.4 eV. Apart from this inclusion of a linear background, the model curve is analogous to that for CF_3^+, and uses the identical internal energy function. The resulting threshold value is $AP_{298}(CF_2OH^+/CF_3OH) \leqslant 13.740 \pm 0.005$ eV ($\leqslant 13.830 \pm 0.005$ eV at 0 K). These, as well as all other thermodynamically relevant values obtained in this work are summarized in Table IV.

C. Photoionization of CF_3OF

Figure 5 provides an overview of the ion yield curves resulting from photoionization of CF_3OF. The relative ion yields reflect the intensities as measured through our quad-

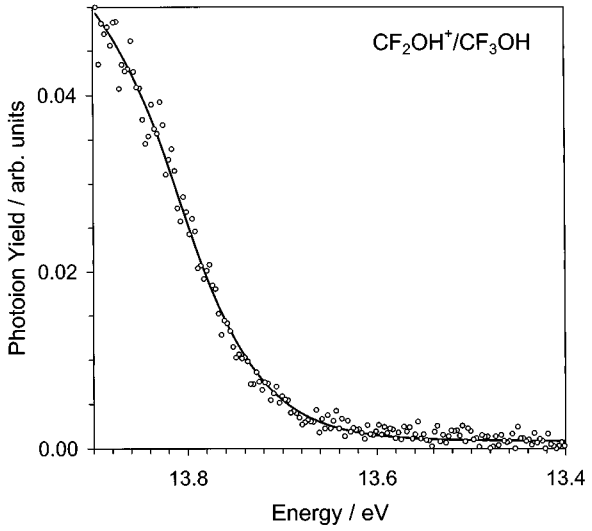

FIG. 4. The threshold region of the CF_2OH^+ fragment from CF_3OH. The solid line is a least-squares fit with a threshold model function (see the text) yielding $AP_0(CF_2OH^+/CF_3OH) \leqslant 13.830 \pm 0.005$ eV.

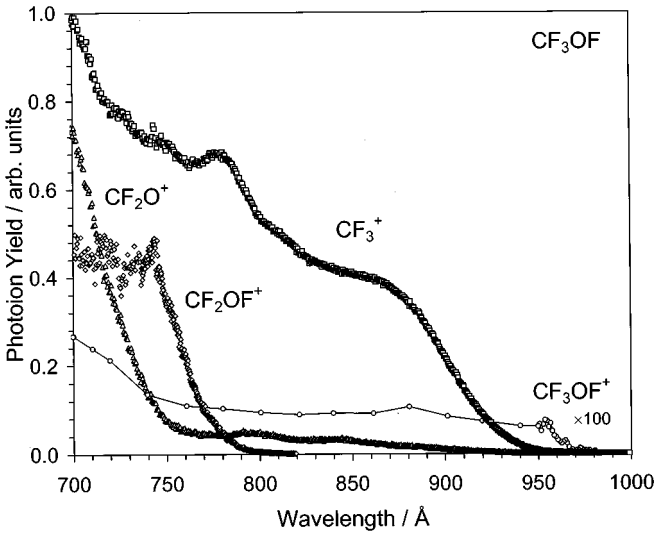

FIG. 5. An overview of the photoion yield curves of the parent CF_3OF^+ and its principal fragments, covering $\sim$ 1000–700 Å. The relative abundances of various ions are correctly depicted in the figure, apart from quadrupole transmission factors. The parent CF_3OF^+ is very weak, but measurable. Discernible in the CF_2O^+ signal as two mild humps (at $\sim$ 800 and $\sim$ 845 Å) is a small contribution from parent ionization of the CF_2O precursor used in the synthesis of CF_3OF and present as a minor impurity. The FCO^+ curve is omitted from this figure, since it was completely attributable to fragmentation from this CF_2O impurity.

rupole mass filter. The most prominent species is the CF_3^+ fragment. The CF_2O^+ curve contains a small contribution from parent ionization of the residual CF_2O precursor used in the synthesis of CF_3OF. The FCO^+ curve was omitted from Fig. 5, because it was completely attributable to fragmentation from the CF_2O impurity.

The parent CF_3OF^+ ion is very weak, but measurable. Immediately following the ionization onset it shows a very brief region of growth, after which it essentially levels off. The threshold region is depicted in more detail in Fig. 6, with points at 0.5 Å intervals. With some prudence due to the weakness of the parent signal, one concludes that the adiabatic ionization onset of CF_3OF is $< 12.782 \pm 0.007$ eV (970.0 ± 0.5 Å), and most likely $\leqslant 12.710 \pm 0.007$ eV (975.5 ± 0.5 Å). This is significantly lower than the value of 13.0 eV listed in the compilation of Lias *et al.*[36] A cusplike feature, centered at 956 ± 1 Å (12.97 ± 0.01 eV), denotes the

TABLE IV. Summary of measured and deduced thermodynamically relevant quantities.

Quantity	298 K	0 K
$IP(CF_3OH)$	⋯	$\leqslant 13.08 \pm 0.05$ eV
$AP(CF_3^+/CF_3OH)$	$\leqslant 13.906 \pm 0.005$ eV	$\leqslant 13.996 \pm 0.005$ eV
$AP(CF_2OH^+/CF_3OH)$	$\leqslant 13.740 \pm 0.005$ eV	$\leqslant 13.830 \pm 0.005$ eV
$IP(CF_3OF)$	⋯	$\leqslant 12.710 \pm 0.007$ eV
		$(< 12.782 \pm 0.007$ eV)
$AP(CF_3^+/CF_3OF)$	$\sim 12.9 \pm 0.1$ eV	$\sim 13.0 \pm 0.1$ eV
	$(< 13.27 \pm 0.10$ eV)	$(< 13.38 \pm 0.10$ eV)
	⋯	$\sim 12.97 \pm 0.01$ eV
$AP(CF_2O^+/CF_3OF)$	$\sim 14.1 \pm 0.1$ eV	$\sim 14.2 \pm 0.1$ eV
$AP(CF_3^+/CF_3OCl)$	$\leqslant 12.736 \pm 0.007$ eV	$\leqslant 12.85 \pm 0.01$ eV
$\Delta H_f^\circ(CF_3OH)$	-217.2 ± 0.9 kcal mol	-215.3 ± 0.9 kcal/mol
$\Delta H_f^\circ(CF_3OF)$	$-176.9^{+1.8}_{-1.3}$ kcal/mol	$-175.5^{+1.8}_{-1.3}$ kcal/mol
	$(> -186.0 \pm 3.4$ kcal/mol)	$(> -184.6 \pm 3.4$ kcal/mol)
$\Delta H_f^\circ(CF_3OCl)$	-175.6 ± 1.0 kcal/mol	-174.2 ± 0.9 kcal/mol
$\Delta H_r^\circ(CF_3OH \rightarrow CF_2O + HF)$	$2.8^{+1.7}_{-1.1}$ kcal/mol	$1.6^{+1.7}_{-1.1}$ kcal/mol
$\Delta H_f^\circ(CF_2OH^+)$	$\leqslant 84.2 \pm 1.0$ kcal/mol	$\leqslant 85.2 \pm 0.9$ kcal/mol
$PA(CF_2O)$	$\geqslant 132.4^{+1.7}_{-1.2}$ kcal/mol	⋯
$D(CF_3O–H)$	$117.5^{+1.9}_{-1.4}$ kcal/mol	$116.4^{+1.9}_{-1.4}$ kcal/mol
$D(CF_3–OH)$	115.2 ± 0.3 kcal/mol	113.9 ± 0.3 kcal/mol
$D(CF_3O–Cl)$	$52.8^{+2.0}_{-1.5}$ kcal/mol	$52.3^{+2.0}_{-1.5}$ kcal/mol
$D(CF_3–OCl)$	88.4 ± 0.3 kcal/mol	87.6 ± 0.3 kcal/mol
$D(CF_3O–H) – D(HO–H)$	$-1.8^{+1.9}_{-1.4}$ kcal/mol	$-1.7^{+1.9}_{-1.4}$ kcal/mol

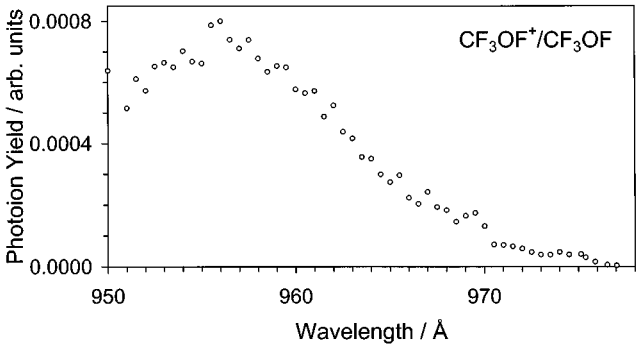

FIG. 6. The threshold region of the parent CF_3OF^+ ion. The growth of this very weak species is terminated in a cusplike structure (956 ± 1 Å) corresponding to the onset of the first fragment, CF_3^+.

termination of the growth of the parent signal and the onset of the CF_3^+ fragment.

Figure 7 depicts the threshold region of the CF_3^+ fragment in greater detail. It should be noted that the fragment curve displays a long tail extending *below* the measurable ionization onset of the parent. Although unusual, this is not entirely surprising, since the internal energy of the neutral CF_3OF should, at least in principle, be available for fragmentation even if the nominal photon energy is below the adiabatic IP. Somewhat more surprising is the appearance of a small humplike structure in the tail region, centered almost exactly at the ionization onset of CF_3OF, ~ 12.70 eV. The origin of this feature is not clearly understood at this time, and perhaps relates to some second-order process.

The solid line in Fig. 7 is an attempted model fit of the experimental data, carried out in a fashion analogous to that

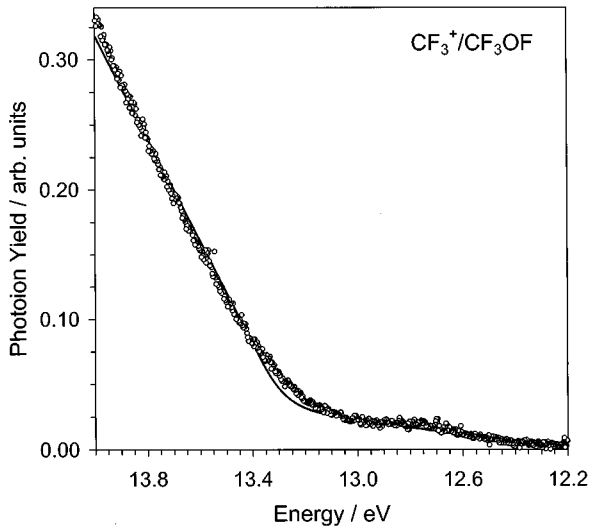

FIG. 7. The threshold region of the CF_3^+ fragment from CF_3OF. The fragment displays a long tail extending below the nominal ionization onset of the parent, and an unusual humplike structure centered at the adiabatic IP of the parent. The solid line is an attempted fit with a threshold model function (see the text) and provides only an upper limit to the AP. The model is unable to reproduce the roundness in the tail, mainly because the fragment yield curve is distorted by unfavorable Franck–Condon factors for parent ionization.

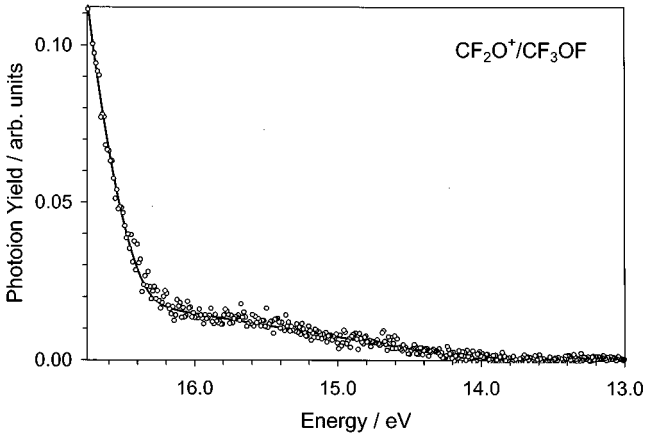

FIG. 8. The shape of the CF_2O^+ fragment yield curve from CF_3OF after subtracting the contribution from the CF_2O impurity. The solid line is an approximate fit (see the text), yielding $AP_0(CF_2O^+/CF_3OF) \approx 14.2 \pm 0.1$ eV.

described in Sec. IV B.[37] Clearly, the fit is far from perfect, and it misses most of the curvature in the tail region. Thus, the fitted threshold value of 13.38 ± 0.10 eV (at 0 K) is just an upper limit to the true value. In all likelihood, the fragmentation threshold is distorted by Frank–Condon factors for parent ionization, as was recently[31] found to be the case in CF_3Cl. This inference is supported by the very small gap between the onsets of the CF_3OF^+ parent and CF_3^+ fragment, and the related weakness of the parent, both of which are even more pronounced than in CF_3Cl.

Given these complications, it appears that a better estimate of the CF_3^+ fragmentation onset can be derived from the position of the cusplike termination of growth of the parent (Fig. 6), found to occur at 12.97 ± 0.01 eV. Another estimate can be obtained from examining the amount of misfit in Fig. 8; this leads to ~ 13.0 ± 0.1 eV. The CF_2O^+ fragment can provide an additional handle on the thermochemistry of CF_3OF. Figure 8 displays the shape of this fragment yield curve, after subtracting the contribution attributable to parent ionization of the CF_2O impurity present in the sample. The amount of correction was determined from the requirement that two broad peaklike structures, visible in Fig. 5 at ~ 845 Å (~ 14.7 eV) and ~ 800 (~ 15.5 eV) and originating from direct ionization of CF_2O, disappear after subtraction of the known[24] parent spectrum. Separately, the related amount of the FCO^+ fragment attributable to ionization of CF_2O was used to reduce the measured FCO^+ signal from the CF_3OF sample; the level of correction for the CF_2O impurity that optimally compensated the humps in the CF_2O^+ ion yield also completely (and rather exactly) canceled the FCO^+ signal recorded from the CF_3OF sample. The corrected CF_2O^+ fragment yield in Fig. 8 displays a low-intensity pseudolinear fragmentation onset, followed by a second, much more pronounced growth at higher energy, which correlates with the termination of growth of the CF_2OF^+ fragment and presumably corresponds to the secondary fragmentation to $CF_2O^+ + 2F$. The weakness of the primary fragmentation process leading to $CF_2O^+ + F_2$, is attributable to steric hindrance, since it requires the concerted

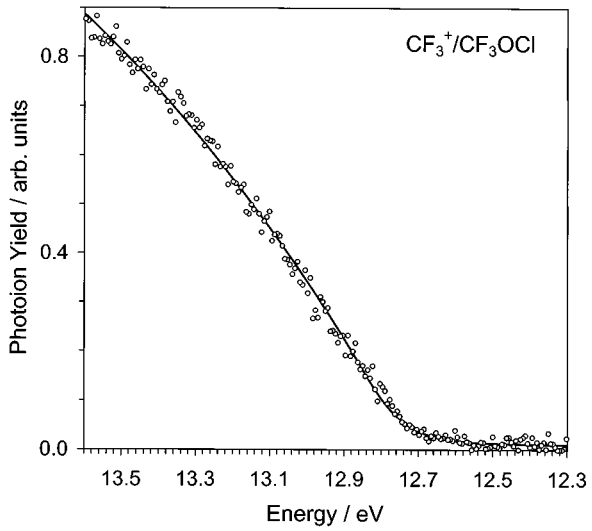

FIG. 9. The threshold region of the CF_3^+ fragment from CF_3OCl. The solid line is a least-squares fit with a threshold model function (see the text), yielding $AP_0(CF_3^+/CF_3OCl) \leqslant 12.85 \pm 0.01$ eV.

elimination of fluorine atoms from opposite ends of the CF_3OF molecule. In addition, the process has to compete with the well-developed fragmentation generating CF_3^+. The solid line in Fig. 8 is an approximate fit by a model function, which incorporates two linear kernels and ''fluctuations'' for the higher energy secondary fragmentation.[24] While the approximate nature of the fit makes the onset of the secondary process highly uncertain, the fit suggests a tentative appearance potential for the primary process of 14.2 ± 0.1 eV (0 K).

D. The CF_3^+ fragment from CF_3OCl

With CF_3OCl we focused our attention primarily on the CF_3^+ fragment ion yield curve, given the deleterious effect that this sample had on our particle multipliers. The parent ionization of CF_3OCl and other fragments were explored only in a very cursory fashion, and no attempt was made to construct an overview spectrum. Nevertheless, it was possible to establish clearly that parent ionization constitutes a significant portion of the total ionization yield, and that CF_3^+ is an early and strong fragment. For example, at the Ne I line (743.7195 Å ≡ 16.671 eV), CF_3^+ appeared to be the most abundant species, while the parent $CF_3O^{35}Cl$ was the next largest signal at about half of that intensity.

Figure 9 displays the threshold region of CF_3^+ from CF_3OCl. The solid line is the model fit, carried out as described above for CF_3OH and CF_3OF. The fitted threshold is $AP_{298}(CF_3^+/CF_3OCl) \leqslant 12.736 \pm 0.007$ eV, corresponding to 12.85 ± 0.01 eV at 0 K.

V. DISCUSSION

A. $\Delta H_f^\circ(CF_3OH)$, $D_0(CF_3-OH)$, and $D_0(CF_3O-H)$

We have recently established[31] that $\Delta H_{f\,0}^\circ(CF_3^+) = 98.1 \pm 0.9$ kcal/mol. With[23] $\Delta H_{f\,0}^\circ(OH) = 9.35 \pm 0.05$ kcal/mol, our $AP(CF_3^+/CF_3OH)$ leads to $\Delta H_{f\,0}^\circ(CF_3OH) \geqslant -215.3 \pm 0.9$ kcal/mol, equivalent to $\Delta H_{f\,298}^\circ(CF_3OH) \geqslant -217.2 \pm 0.9$ kcal/mol. This value is extremely close to several theoretical estimates,[12,13,16,17] but discernibly lower than the estimates based on group additivity properties.[19,20]

Subtracting the best currently available value[31] of $IP(CF_3) = 9.05_5 \pm 0.01_1$ eV from our $AP(CF_3^+/CF_3OH)$ directly yields $D_0(CF_3-OH) \leqslant 113.9 \pm 0.3$ kcal/mol ($\leqslant$ 115.2 ± 0.3 kcal/mol at 298 K). The path to $D(CF_3-OH)$ is more circuitous and requires the knowledge of $\Delta H_f^\circ(CF_3O)$. We have recently recommended[24] $\Delta H_{f\,298}^\circ(CF_3O) = -151.8_{-1.7}^{+1.7}$ kcal/mol, based on our new value[24] for $\Delta H_{f\,298}^\circ(CF_2O) = -149.1_{-0.7}^{+1.4}$ kcal/mol and the room-temperature enthalpy of 21.7 ± 0.9 kcal/mol for the reaction $CF_3O \rightarrow CF_2O + F$ that can be derived from data listed by Batt and Walsh.[20] The latter reaction enthalpy does not appear to be contested, since it is very close to 22.9 ± 2.6 kcal/mol, which is implied by the theoretical[12,17] ΔH_f° values for CF_2O and CF_3O.

With $\Delta H_f^\circ(CF_3OH)$ derived above, the recommended value for $\Delta H_f^\circ(CF_3O)$ leads to $D_{298}(CF_3O-H) = 117.5_{-1.4}^{+1.9}$ kcal/mol (or $116.4_{-1.4}^{+1.9}$ kcal/mol at 0 K), implying that the O–H bond energy in CF_3OH is more than 13 kcal/mol higher than the analogous bond energy in methanol[38] and quite close to the O–H bond in water.[23] In fact, when the error bar is considered, $D_{298}(CF_3O-H) - D_{298}(HO-H) = -1.8_{-1.4}^{+1.9}$ kcal/mol ≈ 0 kcal/mol. The present result is significantly closer to the high bond energy of ~ 120 kcal/mol proposed originally by Wallington *et al.*[7] than to the low value of ~ 109 kcal/mol suggested by Benson.[19] The relatively high bond energy suggests that CF_3OH is a reasonably good sink for stratospheric CF_3O. However, since it seems that nominally $D(HO-H) \geqslant D(CF_3O-H)$, reaction with OH radicals may be capable of recycling CF_3O from CF_3OH.

The value of $\Delta H_f^\circ(CF_3OH)$ derived above also implies that at 298 K the reaction enthalpy for the 1,2-elimination of HF is $2.8_{-1.1}^{+1.7}$ kcal/mol ($1.6_{-1.1}^{+1.7}$ kcal/mol at 0 K). This, as well as other thermodynamical values derived in this work are summarized in Table IV.

B. $\Delta H_f^\circ(CF_2OH^+)$

Combining $\Delta H_f^\circ(CF_3OH)$ determined above and $AP(CF_2OH^+/CF_3OH)$ leads to $\Delta H_{f\,0}^\circ(CF_2OH^+) \leqslant 85.2 \pm 0.9$ kcal/mol (or 84.2 ± 1.0 kcal/mol at 298 K). This is ~ 32 kcal/mol higher than the heat of formation (52 kcal/mol) listed by Lias *et al.*[36] and derived from the generally accepted value for the proton affinity[39] $PA(CF_2O) = 160.5$ kcal/mol (based on measurements by McMahon and collaborators[40]) and the JANAF[22] value for $\Delta H_f^\circ(CF_2O)$. Using the new[24] $\Delta H_f^\circ(CF_2O)$ instead of the tabulated value, we obtain 56.1 ± 2 kcal/mol (298 K) for the heat of formation of protonated carbonyl fluoride, still 28.1 kcal/mol lower than the value implied by $AP(CF_2OH^+/CF_3OH)$.

Technically, experimental fragmentation thresholds are upper limits to the true values, and therefore the discrepancy is in the allowed direction. However, the shape of the ion yield curve and the quality of the threshold fit in Fig. 4

suggest that our value is more than just a coarse upper limit. The only hint for a possible existence of a lower energy fragmentation process is the weak sloping tail extending to lower energy. The shape of the threshold suggests that the fragmentation either does not involve rearrangement, or that such rearrangement is unusually facile and efficient. In the absence of rearrangement, the isomeric structure most likely generated by the fragmentation of CF_3OH^+ is CF_2OH^+, corresponding to a simple bond scission.

The massive discrepancy between the values of $\Delta H_f^\circ(CF_2OH^+)$, as obtained from $AP(CF_2OH^+/CF_3OH)$ or $PA(CF_2O)$ is puzzling. The heat of formation of CF_2OH^+ implied by $PA(CF_2O)$ is such that fragmentation of CF_3OH would have to commence at $\sim$ 12.6 eV, below the observable ionization threshold. Consequently, one would expect the parent to be very weak and the primary process at the adiabatic ionization onset to be the appearance of the CF_2OH^+ fragment. This is clearly not the case here. One possible explanation is that the CF_2OH^+ asymptote is not readily reachable from the CF_3OH^+ manifold accessible by direct ionization, perhaps because of a barrier. In this case the measured onset of CF_2OH^+ would correspond either to the top of the barrier or to some suitable excited state of CF_2OH^+, which effectively opens a new dissociation asymptote. A slight variation on this theme is that the observed fragmentation processes and the PA experiments access different isomers of protonated carbonyl fluoride.

In order to shed some more light on this situation, we have performed exploratory *ab initio* calculations at the MP2/6-31G(d,p) level. These were unable to indicate any singlet or triplet structures that would be lower in energy than CF_2OH^+. Instead, a structure corresponding to FCO^+ with an HF moiety roughly perpendicular to it and $\sim$ 2.2 Å away (C–F distance), was found to represent a minimum on the potential energy surface roughly midway between the most stable CF_2OH^+ structure and the $FCO^+ + HF$ asymptote. However, even if the observed threshold corresponds to such an adduct, it is not apparent why the fragmentation pathways of CF_3OH^+ would ignore the generation of CF_2OH^+ by a simple bond scission. Clearly, a more elaborate theoretical study of the CF_3OH^+ and CF_2OH^+ systems is needed before a definitive answer can be given.

C. $\Delta H_f^\circ(CF_3OF)$

The fitted appearance potential of the CF_3^+ fragment from CF_3OF obtained in Sec. IV C is only an upper limit to the true value. Using[23,41] $\Delta H_{f\,0}^\circ(OF) = 25.9 \pm 2.3$ kcal/mol leads to $\Delta H_{f\,0}^\circ(CF_3OF) > -184.6 \pm 3.4$ kcal/mol. JANAF[22] lists $-$ 180.8 $\pm$ 3.1, but their value was derived by reference to $\Delta H_f^\circ(CF_2O)$, which has since been shown[24] to be too low by at least 4 kcal/mol. Also, there appears to be a problem[37] with JANAF's correction from 298 to 0 K.

A better approach to $\Delta H_f^\circ(CF_3OF)$ is to use experimental data evaluated by Batt and Walsh,[20] which can be combined[42] to give the reaction enthalpy at 298 K for $CF_3OF \rightarrow CF_2O + F_2$ of 27.8 $\pm$ 1.1 kcal/mol, somewhat lower than the 30.1 $\pm$ 3 kcal/mol adopted by JANAF.[22] Our approximate $AP_0(CF_2O^+/CF_3OF) \approx 14.2 \pm 0.1$ eV, when coupled with[24] $IP(CF_2O) = 13.024 \pm 0.004$ eV, yields 28 $\pm$ 2 kcal/mol, further corroborating the reaction enthalpy derived from Batt and Walsh.[20] This yields $\Delta H_{f\,298}^\circ(CF_3OF) = -176.9^{+1.8}_{-1.3}$ kcal/mol, or $-$ $175.5^{+1.8}_{-1.3}$ kcal/mol at 0 K, over 5 kcal/mol higher than the JANAF[22] value. Using this heat of formation of CF_3OF, one obtains $AP_0(CF_3^+/CF_3OF) = 12.99 \pm 0.13$ eV, significantly lower than our fitted upper limit of 13.4 $\pm$ 0.1 eV, but very close to the estimates based either on the amount of misfit in Fig. 7 or on the position of the cusplike structure in the parent CF_3OF^+ ion yield (Fig. 6).

D. $\Delta H_f^\circ(CF_3OCl)$

Our $AP_0(CF_3^+/CF_3OCl)$, with the well established[22,23] $\Delta H_{f\,0}^\circ(OCl) = 24.15 \pm 0.03$ kcal/mol yields $\Delta H_{f\,0}^\circ(CF_3OCl) \geqslant -174.2 \pm 0.9$ kcal/mol, equivalent to -175.6 ± 1.0 kcal/mol at 298 K. This in turn leads to $D_0(CF_3O–Cl) \leqslant 52.3^{+2.0}_{-1.5}$ kcal/mol ($52.8^{+2.0}_{-1.5}$ kcal/mol at 298 K), which compares very well with the upper limit of $<$ 53 kcal/mol determined experimentally by Rengarajan *et al.*[43] The value of $AP_0(CF_3^+/CF_3OCl)$, when combined with $IP(CF_3)$, produces $D_0(CF_3–OCl) \leqslant 87.6 \pm 0.3$ kcal/mol, equivalent to 88.4 $\pm$ 0.3 kcal/mol at 298 K.

VI. CONCLUSIONS

Our study of CF_3OH by photoionization mass spectrometry yields $IP(CF_3OH) \leqslant 13.08 \pm 0.05$ eV, and, by accurate fitting of the fragmentation threshold regions, $AP_0(CF_3^+/CF_3OH) \leqslant 13.996 \pm 0.005$ eV and $AP_0(CF_2OH^+/CF_3OH) \leqslant 13.830 \pm 0.005$ eV. The appearance potential of the CF_3^+ fragment from CF_3OH proves useful in deriving $\Delta H_{f\,298}^\circ(CF_3OH) \geqslant -217.2 \pm 0.9$ kcal/mol, corroborating recently calculated *ab initio* values[12,13,16,17] for this quantity. Together with $IP(CF_3) = 9.05_5 \pm 0.01_1$ eV, it also implies $D_{298}(CF_3–OH) \leqslant 115.2 \pm 0.3$ kcal/mol. Using the recently[24] recommended $\Delta H_f^\circ(CF_2O)$ the present value of $\Delta H_f^\circ(CF_3OH)$ leads to a reaction enthalpy for the 1,2-elimination of HF of $\Delta H_{r\,298}^\circ = 2.8^{+1.7}_{-1.1}$ kcal/mol ($1.6^{+1.7}_{-1.1}$ kcal/mol at 0 K).

Combining $\Delta H_f^\circ(CF_3OH)$ with $\Delta H_f^\circ(CF_3O)$ derived previously,[24] leads to $D_{298}(CF_3O–H) = 117.5^{+1.9}_{-1.4}$ kcal/mol. This is significantly closer to the high bond value originally proposed by Wallington *et al.*,[7] and backed by several *ab initio* calculations,[12,14,17,18] than to the low value of $\sim$109 kcal/mol suggested by Benson[19] on the basis of group additivity estimates. When error bars are included, then $D_{298}(CF_3O–H) - D_{298}(HO–H) = -1.8^{+1.9}_{-1.4}$ kcal/mol ≈ 0 kcal/mol. However, if one disregards the error bars, then $D(CF_3O–H)$ is nominally slightly lower than $D(HO–H)$. This is in contrast to the original conclusion by Wallington *et al.*,[7] but perhaps in good accord with the more recent observation that CF_3O does not appear to give rise to appreciable hydrogen abstraction from water.[8]

The appearance potential of CF_2OH^+ from CF_3OH leads to $\Delta H_{f\,298}^\circ(CF_2OH^+) \leqslant 84.2 \pm 1.0$ kcal/mol, which is

$\sim$28 kcal/mol higher than the value deduced from $PA(CF_2O)$, and may correspond to a different structure.

Photoionization of CF_3OF produces a very weak parent, with an apparent adiabatic $IP(CF_3OF) \leqslant 12.710 \pm 0.007$ eV, significantly lower than previous values derived by photoelectron spectroscopy.[36] The threshold region of the CF_3^+ fragment from CF_3OF is suppressed by unfavorable Franck–Condon factors for parent ionization, and a direct fit establishes only an upper limit of $AP_0(CF_3^+/CF_3OF) < 13.38 \pm 0.10$ eV. However, the cusplike termination of growth in the CF_3OF^+ parent ion, at $\sim$ 12.97 $\pm$ 0.01 eV, provides a better estimate for the onset of the CF_3^+ fragment and is compatible with the value of $\Delta H^\circ_{f\,298}(CF_3OF) = -176.9^{+1.8}_{-1.3}$ kcal/mol proposed here on the basis of other arguments, which include an approximate determination of $AP_0(CF_2O^+/CF_3OF) \approx 14.2 \pm 0.1$ eV. The latter appearance potential is in excellent agreement with the reaction enthalpy for $CF_3OF \rightarrow CF_2O + F_2$ of 27.8 $\pm$ 1.1 kcal/mol (298 K), which can be derived from data evaluated by Batt and Walsh.[20]

The fitted value for the appearance potential of CF_3^+ from CF_3OCl, $AP_0(CF_3^+/CF_3OCl) \leqslant 12.85 \pm 0.01$ eV, leads to $\Delta H^\circ_{f298}(CF_3OCl) \geqslant -175.6 \pm 1.0$ kcal/mol, $D_{298}(CF_3\text{–}OCl) \leqslant 88.4 \pm 0.3$ kcal/mol, and $D_{298}(CF_3O\text{–}Cl) \leqslant 52.8^{+2.0}_{-1.5}$ kcal/mol. The latter value is in very good agreement with the upper limit of <53 kcal/mol determined recently by Rengarajan *et al.*[43]

ACKNOWLEDGMENT

This work was supported by the U.S. Department of Energy, Office of Basic Energy Sciences, under Contract No. W-31-109-ENG-38.

[1] (a) World Meteorological Organization Global Ozone Research and Monitoring Project, Report No. 20, UN Environment Program, WMO, Geneva, 1990; (b) World Meteorological Organization Global Ozone Research and Monitoring Project, Report No. 25, UN Environment Program, WMO, Geneva, 1992.

[2] (a) M. J. Molina and F. S. Rowland, Nature **249**, 810 (1974); (b) R. S. Stolarski and R. D. Rundel, Geophys. Res. Lett. **2**, 443 (1975).

[3] See, for example, E. W. Kaiser, T. J. Wallington, and M. D. Hurley, Int. J. Chem. Kinet. **27**, 205 (1995), and references therein.

[4] (a) M. K. W. Ko, *et al.*, Geophys. Res. Lett. **21**, 101 (1994); (b) A. R. Ravishankara, A. A. Turnipseed, N. R. Jensen, S. B. Barone, M. Mills, C. J. Howard, and S. Solomon, Science **71**, 263 (1994).

[5] See, for example: R. Meller and G. K. Moortgat, J. Photochem. Photobiol. A: Chem. **86**, 15 (1995), and references therein.

[6] See, for example, T. J. Wallington and J. C. Ball, J. Phys. Chem. **99**, 3201 (1995), and references therein.

[7] T. J. Wallington, M. D. Hurley, W. F. Schneider, J. Sehested, and O. J. Nielsen, J. Phys. Chem. **97**, 7606 (1993).

[8] A. A. Turnipseed, S. B. Barone, N. R. Jensen, D. R. Hanson, C. J. Howard, and A. R. Ravishankara, J. Phys. Chem. **99**, 6000 (1995).

[9] L. G. Huey, D. R. Hanson, and E. R. Lovejoy, J. Geophys. Res. **100**, 18771 (1995); (b) W. F. Schneider, T. J. Wallington, and R. E. Huie, J. Phys. Chem. **100**, 6097 (1996).

[10] (a) W. F. Schneider, T. J. Wallington, K. Minschwaner, and E. A. Stahlberg, Environ. Sci. Technol. **29**, 247 (1995); (b) L. T. Molina and M. J. Molina, Geophys. Res. Lett. **23**, 563 (1996).

[11] (a) E. R. Lovejoy, L. G. Huey, and D. R. Hanson, J. Geophys. Res. **100**, 18775 (1995); (b) L. G. Huey, P. W. Villalta, E. J. Dunlea, D. R. Hanson, and C. J. Howard, J. Phys. Chem. **100**, 190 (1996).

[12] W. F. Schneider and T. J. Wallington, J. Phys. Chem. **97**, 12783 (1993).

[13] M. Sana, G. Leroy, D. Peters, and C. Willante, J. Mol. Struct. (Theochem.) **164**, 249 (1988).

[14] D. A. Dixon and R. Fernandez, Proceedings of the STEP-HALOCSIDE AFEAS Workshop, Dublin, Ireland, March 1993 (unpublished).

[15] (a) C. W. Bock, M. Trachtman, H. Niki, and G. J. Mains, J. Phys. Chem. **98**, 7976 (1994); (b) W. F. Schneider and T. J. Wallington, *ibid*. **99**, 4353 (1995); (c) C. W. Bock, M. Trachtman, H. Niki, and G. J. Mains, *ibid*. **99**, 4354 (1995).

[16] (a) J. A. Montgomery, Jr., H. H. Michels, and J. S. Francisco, Chem. Phys. Lett. **220**, 391 (1994); (b) J. S. Francisco, *ibid*. **218**, 401 (1994); (c) Chem. Phys. **150**, 19 (1991).

[17] W. F. Schneider and T. J. Wallington, J. Phys. Chem. **98**, 7448 (1994).

[18] W. F. Schneider, T. J. Wallington, and M. D. Hurley, J. Phys. Chem. **98**, 2217 (1994); W. F. Schneider, B. I. Nance, and T. J. Wallington, J. Am. Chem. Soc. **117**, 478 (1995).

[19] S. W. Benson, J. Phys. Chem. **98**, 2216 (1994).

[20] (a) L. Batt and R. Walsh, Int. J. Chem. Kinet. **14**, 933 (1982); (b) **15**, 605 (1983).

[21] W. F. Schneider, T. J. Wallington, and M. D. Hurley, J. Phys. Chem. **98**, 2217 (1994).

[22] M. W. Chase, C. A. Davies, J. R. Downey, Jr., D. J. Frurip, R. A. McDonald, and A. N. Syverud, *JANAF Thermochemical Tables*, 3rd ed. [J. Phys. Chem. Ref. Data **14**, Suppl. 1 (1985)].

[23] L. V. Gurvich, I. V. Veyts, and C. B. Alcock, *Thermodynamic Properties of Individual Substances* (Hemisphere, New York, 1991), Vols. 1 and 2.

[24] R. L. Asher, E. H. Appelman, and B. Ruscic, J. Chem. Phys. **105**, 9781 (1996).

[25] L. A. Curtiss, K. Raghavachari, C. P. Redfern, and J. A. Pople, J. Chem. Phys. **106**, 1063 (1997).

[26] (a) K. Seppelt, Angew. Chem. Int. Ed. Engl. **16**, 322 (1977); (b) G. Klöter and K. Seppelt, J. Am. Chem. Soc. **101**, 347 (1979).

[27] (a) D. E. Gould, L. R. Anderson, D. E. Young, and W. B. Fox, J. Am. Chem. Soc. **91**, 1310 (1969); (b) C. J. Schack and W. Maya, *ibid*. **91**, 2902 (1969); (c) M. Lustig, A. R. Pitochelli, and J. K. Ruff, *ibid*. **89**, 2841 (1967).

[28] M. J. Frisch, G. W. Trucks, M. Head-Gordon, P. M. W. Gill, M. W. Wong, J. B. Foresman, B. G. Johnson, H. B. Schlegel, M. A. Robb, E. S. Replogle, R. Gomperts, J. L. Andres, K. Raghavachari, J. S. Binkley, C. Gonzalez, R. L. Martin, D. J. Fox, D. J. Defrees, J. Baker, J. J. P. Stewart, and J. A. Pople, GAUSSIAN 94, Rev. D. 1 (Gaussian Inc., Pittsburgh, PA, 1994).

[29] P. C. Hariharan and J. A. Pople, Theor. Chim. Acta **28**, 213 (1968).

[30] (a) B. Ruscic and J. Berkowitz, J. Phys. Chem. **97**, 11451 (1993); (b) J. Chem. Phys. **100**, 4498 (1994); (c) **101**, 7795 (1994); (d) **101**, 7975 (1994); (e) **101**, 10936 (1994).

[31] R. L. Asher and B. Ruscic, J. Chem. Phys. **106**, 210 (1997).

[32] P. C. Haarhoff, Mol. Phys. **7**, 101 (1963).

[33] P. M. Wilt and E. A. Jones, J. Inorg. Nucl. Chem. **30**, 2933 (1968).

[34] Since Haarhoff's expression (Ref. 32) does not readily accommodate a hindered internal rotor, which would have been the most appropriate description for the internal energy associated with the CF_3 torsion in CF_3OH, CF_3OF, and CF_3OCl, two versions of the internal energy distribution were developed: one treated the internal rotation as a pseudovibration, and the other treated it as a free internal rotation. In all three cases the difference between the two variations was only minor, and employment of either approach gave similar overall answers. The final fits were performed using the pseudovibrator approach, which appeared to provide a slightly better description of the internal energy distribution than the free rotor model.

[35] See, for example, B. Ruscic, J. Chem. Phys. **85**, 3776 (1986); *Modelling of Structure and Properties of Molecules*, edited by Z. B. Maksic (Horwood, Chichester, 1987), pp. 221–238.

[36] S. G. Lias, J. E. Bartmess, J. F. Liebman, J. L. Holmes, R. D. Levin, and W. G. Mallard, J. Phys. Chem. Ref. Data **17**, Suppl. 1 (1988).

[37] While preparing the function for this fit, an interesting discrepancy has surfaced. JANAF (Ref. 22) states that it uses a hindered rotor approach and spectroscopic data of Wilt and Jones (Ref. 33) to calculate the thermodynamic properties of CF_3OF, and it lists 3.500 kcal/mol for $H_{298} - H_0$. Using the same data, we obtain 4.081 kcal/mol from the hindered rotor approach. The more straightforward pseudovibrator approach ($56\ cm^{-1}$) yields an almost identical 4.060 kcal/mol for the same quantity. The internal energy function used in our fits was constrained to corre-

spond to the available internal energy that results from the hindered rotor approach.

[38] (a) D. L. Osborn, D. J. Leahy, E. M. Ross, and D. M. Newmark, Chem. Phys. Lett. **235**, 484 (1995); (b) M. Meot-Ner (Mautner) and L. W. Sieck, J. Phys. Chem. **90**, 6687 (1986); (c) P. C. Engelking, G. B. Ellison, and W. C. Lineberger, J. Chem. Phys. **69**, 1826 (1978); (d) J. D. Garcia and J. E. Mack, J. Opt. Soc. Am. **55**, 654 (1965); (e) B. Ruscic and J. Berkowitz, J. Chem. Phys. **95**, 4033 (1991).

[39] S. G. Lias, J. F. Liebman, and R. D. Levin, J. Phys. Chem. Ref. Data **13**, 695 (1984).

[40] (a) S. M. Collyer and T. B. McMahon, J. Phys. Chem. **87**, 909 (1983); (b) C. E. Doiron and T. B. McMahon, Can. J. Chem. **59**, 2689 (1981).

[41] J. Berkowitz, P. M. Dehmer, and W. A. Chupka, J. Chem. Phys. **59**, 925 (1973).

[42] Batt and Walsh (Ref. 20) list the following reaction enthalpies: $\Delta H^{\circ}_{r\,298}(\mathrm{a}) = 24.5 \pm 0.7$ kcal/mol for $CF_3OOCF_3 \rightarrow CF_3OF + CF_2O$, $\Delta H_{r\,298}(\mathrm{b}) = 46.8 \pm 0.5$ kcal/mol for $CF_3OOCF_3 \rightarrow 2CF_3O$, and $\Delta H^{\circ}_{r\,298}(\mathrm{c}) = 44.0$ kcal/mol (presumably also $\pm$ 0.5 kcal/mol) for $CF_3OF \rightarrow CF_3O + F$. The reaction enthalphy for $CF_3OF \rightarrow CF_2O + F_2$ at 298 K is then $2\Delta H^{\circ}_{r\,298}(\mathrm{c}) - \Delta H^{\circ}_{r\,298}(\mathrm{b}) + \Delta H^{\circ}_{r\,298}(\mathrm{a}) - D_{298}(F_2)$, or 27.8 $\pm$ 1.1 kcal/mol.

[43] R. Rengarajan, D. W. Setser, and D. D. DesMarteau, J. Phys. Chem. **98**, 10568 (1994).